

Tetrachloroferrate(III) Complexes of some Organic Diammonium Cations: Structures and Magnetic Properties

Bruce D. James^{a,*}, Jerzy Mrozinski^{b,*}, Julia Klak^b, Brian W. Skelton^c, and Allan H. White^c

^a Bundoora/Victoria / Australia, La Trobe University, Department of Chemistry

^b Wrocław/Poland, University of Wrocław, Department of Chemistry.

^c Crawley/Western Australia, University of Western Australia, School of Biomedical, Biomolecular and Chemical Sciences, Chemistry M313

Received July 3rd, 2007.

Abstract. With aqueous acidic iron(III) chloride, the three diamines ethylenediamine (en), tetramethylethylenediamine (tmeda) and 4:4'-tetramethyldiaminodiphenylmethane (ddmp) yield the aquapentachloroferrate(III) and a pair of $[\text{FeCl}_4]^- \text{Cl}^-$ double salts, respectively. Their structures indicate that N–H···Cl hydrogen bonding is present, but the Fe···Fe distances are all quite long. The magnetic data show that, while all the materials display antiferro-

magnetic coupling on cooling, in none of the cases was any transition observed above 1.8 K.

Keywords: Iron; Aquapentachloroferrate(III); Ethylenediammonium salt; Tetrachloroferrate(III) double salts; Tetramethylethylenediammonium; 4:4'-Tetramethyldiammoniumdiphenylmethane; Crystal structures; Magnetic properties

Introduction

Tetrachloroferrate(III) compounds are well known [1] and are of interest because the weak-field chloride ligands permit the maximum spin state for a d^5 electronic configuration [2]. It has been found, however, that synthetic results are not always straightforward and that different counterions may produce compounds having different compositions. Some of the materials having more unusual anion compositions such as $[\text{Fe}_2\text{Cl}_9]^{3-}$ can contain the $[\text{FeCl}_4]^-$ anion [3], an observation quite consistent with the stability of that species, particularly in acidic solution [4]. On the other hand, the classic compound $(\text{NH}_4)_2[\text{FeCl}_5(\text{OH}_2)]$ contains a (distorted) octahedral Fe^{III} ion [5], even though it is also obtained from an acidic solution.

Extensive studies by *Carlin's* group have shown that systems based on pyridinium and substituted pyridinium cations (pyH^+) are able to form hydrogen-bonded ion clusters, effectively $[(\text{pyH})_3\text{Cl}]^{2+}$, that can function as cations to stabilize chloroferrate(III) compounds [6]. Some quinolinium

cations, however, may yield other double salts, the structures of which may depend on the position of substituents in the heterocyclic system [7].

Chloroferrate(III) derivatives of diammonium cations appear to have received little attention, and structural information is consequently sparse. The compound formed from iron(III) chloride and the simplest diamine, 1,2-diaminoethane (ethylenediamine, en) was reported in 1926, albeit with reservations about the presence of the aqua ligand [8], while the hexanediammonium system appears to be the only other one that has been characterized, and this yielded an interesting mix of ions [9]. Consequently, it was considered that a comparison of the chloroferrates derived from diamines having small carbon chains and synthesized under similar (aqueous acidic) conditions might prove to be interesting in terms of possible interplay between double salt formation, increased coordination number about the iron ion, and any significant influences of hydrogen-bonding in their structures. The diamines chosen were the two-carbon backbone ethylenediamine (en) and 1,1,2,2-tetramethylethylenediamine (tmeda) and the one-carbon, but phenyl-substituted (and sterically-significant) 4:4'-tetramethyldiaminodiphenylmethane (ddmp). The structures and magnetic properties of the materials are described here.

Experimental Section

Syntheses

4:4'-Tetramethyldiaminodiphenylmethane (ddmp) was a BDH product, while other reagents were obtained from the Aldrich Chemical Co. All were employed without further purification.

Syntheses were based on similar ones previously described [3, 5, 7, 9], and generally carried out in about 10^{-2} mole quantities. In gen-

* Dr. Bruce D. James
Department of Chemistry, La Trobe University
Vic. 3086, Australia.
Tel.: +61 3 9479 2534
Fax.: +61 3 9479 1399
E-mail: b.james@latrobe.edu.au

* Prof. Dr. Jerzy Mrozinski
Faculty of Chemistry, University of Wrocław, F. Joliot – Curie 14
PL-50-383 Wrocław, Poland
Tel.: +48 71 375 7307
Fax.: +48 71 328 2348
E-mail: jmroz@wchuwr.chem.uni.wroc.pl

eral, the base was dissolved in ethanol (with warming and additional hydrochloric acid where necessary) and the solution added slowly with constant stirring to an approximately equimolar quantity of hydrated iron(III) chloride dissolved separately in an excess of aqueous HCl. Sufficient conc. aqueous HCl or ethanol was added (with further warming as necessary) to dissolve any precipitated solids, and the resulting solution was allowed to evaporate slowly in an air stream until crystals appeared (generally several days). Products: (tmedaH₂)[FeCl₄]Cl (**1**), yellow crystals, mp. 195–197; (ddmpH₂)[FeCl₄]Cl (**2**), yellow crystals, m.p. 175–177; (enH₂)[FeCl₅(OH₂)] (**3**), dark red-brown crystals, m.p. 109–110 °C

Analyses (Campbell Microanalytical Laboratory, University of Otago, New Zealand):

Calcd for (tmedaH₂)[FeCl₄]Cl: C, 20.51; H, 5.16; N, 7.97; Cl, 50.46. Found: C, 20.47; H, 5.08; N, 7.89; Cl, 50.31 %.

Calcd. for (ddmpH₂)[FeCl₄]Cl: C, 41.71; H, 4.94; N, 5.72; Cl, 36.22. Found: C, 41.78; H, 5.22; N, 5.91; Cl, 36.22 %

Calcd. for (enH₂)[FeCl₅(OH₂)]: C, 7.43; H, 3.74; N, 8.66; Cl, 54.84. Found: C, 7.36; H, 3.80; N, 8.34; Cl, 53.51 %

Structure determinations

Full spheres of CCD area-detector diffractometer data were measured (ω -scans; monochromatic Mo K α radiation; λ = 0.71073 Å), yielding $N_{\text{(total)}}$ reflections, these merging to N unique (R_{int} cited) after 'empirical'/multiscan absorption correction (proprietary software), N_{o} with $I > 2\sigma(I)$ being considered 'observed'. Full matrix least squares refinement on F^2 refined anisotropic displacement parameters for the non-hydrogen atoms, hydrogen atoms being included constrained according to a riding model (reflection weights: $(\sigma^2(F^2) + (aP)^2 + (bP))^2$ ($P = (F_{\text{o}} + 2F_{\text{c}})/3$)). Neutral atom complex scattering factors were employed within the SHELXL-97 program [10]. Pertinent results are given below and in the Tables and Figures, the latter showing 20 % (room-temperature) and 50 % (low-temperature) probability amplitude displacement ellipsoids for the non-hydrogen atoms, hydrogen atoms having arbitrary radii of 0.1 Å. Individual variations in procedure are cited as 'variata'. Crystallographic data for the structures have been deposited with the Cambridge Crystallographic Data Centre, CCDC 633029-633030, 643244. Copies can be obtained free of charge on application to The Director, CCDC, 12 Union Road, Cambridge CB2 1EZ, UK (Fax: int.code + (1223)336-033; e-mail for inquiry: fileserv@ccdc.cam.ac.uk; email for deposition: deposit@ccdc.cam.ac.uk).

Crystallrefinement data

1. (tmedaH₂)[FeCl₄]Cl (1**)** \equiv C₆H₁₈Cl₅FeN₂, M = 351.3. Monoclinic, space group $P2_1/n$ (C_{2h}^5 , No. 14 (variant)), a = 6.7973(2), b = 19.0746(4), c = 12.1794(3) Å, β = 102.453(2)°, V = 1542 Å³. D_{c} (Z = 4) = 1.51₃ g cm⁻³. μ_{Mo} = 1.82 mm⁻¹; specimen: 0.32 × 0.17 × 0.12 mm; $T_{\text{min/max}}$ = 0.87. $2\theta_{\text{max}}$ = 70°; N_{t} = 21369, N = 6264 (R_{int} = 0.033), N_{o} = 3783; $R1$ = 0.033, $wR2$ = 0.075 (a = 0.0312); S = 1.02. $|\Delta\rho_{\text{max}}|$ = 0.58 e Å⁻³. T ca. 100 K

2. (ddmpH₂)[FeCl₄]Cl (2**)** \equiv C₁₇H₂₄Cl₅FeN₂, M = 489.5. Monoclinic, space group $P2_1/n$ (C_{2h}^5 , No. 14 (variant)), a = 13.184(2), b = 13.832(3), c = 14.636(2) Å, β = 116.732(2)°, V = 2384 Å³. D_{c} (Z = 4) = 1.36₄ g cm⁻³. μ_{Mo} = 1.20 mm⁻¹; specimen: 0.55 × 0.35

× 0.30 mm; $T_{\text{min/max}}$ = 0.83. $2\theta_{\text{max}}$ = 58°; N_{t} = 27745, N = 5991 (R_{int} = 0.023), N_{o} = 3619; $R1$ = 0.036, $wR2$ = 0.110 (a = 0.0638); S = 1.05. $|\Delta\rho_{\text{max}}|$ = 0.39 e Å⁻³. T ca. 298 K

Variata. The anion was modelled as rotationally disordered about Fe-Cl(11), site occupancies of the two sets of chlorine atoms refining to 0.57(2) and complement. Data were measured at room-temperature.

3. (enH₂)[FeCl₅(OH₂)] (3**)** \equiv C₂H₁₂Cl₅FeN₂O, M = 313.2. Orthorhombic, space group $P2_12_12_1$ (D_{2h}^4 , No. 19), a = 6.8796(6), b = 10.7140(10), c = 14.3471(9) Å, V = 1057 Å³. D_{c} (Z = 4) = 1.96₇ g cm⁻³. μ_{Mo} = 2.6 mm⁻¹; specimen: 0.32 × 0.30 × 0.24 mm; $T_{\text{min/max}}$ = 0.82. $2\theta_{\text{max}}$ = 82°; N_{t} = 77754, N = 6874 (R_{int} = 0.025), N_{o} = 6436; $R1$ = 0.023, $wR2$ = 0.057 (a = 0.0250, b = 0.1435); S = 1.40. x_{abs} = 0.377(7). $|\Delta\rho_{\text{max}}|$ = 0.69 e Å⁻³. T ca. 100 K

Variata. The high value of x_{abs} appears to be consequent on the quasi-centrosymmetric nature of the structure (rather than twinning or other problems).

Magnetic measurements

The magnetization of the powdered samples was measured over the temperature range 1.8–300 K using a Quantum Design SQUID-based MPMSXL-5-type magnetometer. The superconducting magnet could be operated at a field strength ranging from 0 to 5 T. Measurements on the sample compounds were made at magnetic field 0.5 T. The SQUID magnetometer was calibrated with a palladium rod sample. Corrections are based on subtracting the sample-holder signal and contribution χ_{D} estimated from Pascal constants [11] which are -240×10^{-6} cm³mol⁻¹ for the complex (tmedaH₂)[FeCl₄]Cl (**1**), -185×10^{-6} cm³mol⁻¹ for (ddmpH₂)[FeCl₄]Cl (**2**), and, finally, -147×10^{-6} cm³mol⁻¹ for (enH₂)[FeCl₅(OH₂)] (**3**). The effective magnetic moment was calculated from the equation, $\mu_{\text{eff}} = 2.83(\chi_{\text{M}}T)^{1/2}$ (B.M.).

EPR spectra

EPR spectra were recorded at room temperature and at 77 K on a Bruker ESP 300 spectrometer operating at X-band, and equipped with an ER 035M Bruker NMR gaussmeter and HP 5350B Hewlett-Packard microwave frequency counter. The spectra at 4.5 K temperature were measured with an X-band Radiopan SE/X 2543 Spectrometer

Results and Discussion

Structures

The results of the single crystal X-ray structure determinations are all consistent with the proposed compositions and connectivities implied above, being the salt [FeCl₅(OH₂)]²⁻ (in **3**) or double salts ([FeCl₄]⁻ · Cl⁻) (**1**, **2**) of the relevant organic cations. The structures of the [FeCl₄]⁻ species are essentially as expected, and are shown in the figure captions.

1. (tmedaH₂)[FeCl₄]Cl (1**).** Here, a full formula unit, devoid of crystallographic symmetry, comprises the asymmetric unit of the structure (Figure 1(a)). Interactions of the

protonic hydrogen atoms are with the uncoordinated chloride ions, forming a strand along and parallel to *a*: Cl1...N,H2 3.045(5), 2.2; ...N,H1 (*x*−1, *y*, *z*) 3.040(5), 2.1 Å (N-H...Cl 167, 158° respectively, H...Cl...H *ca.* 132°) (Figure 1(b)), the chlorine atoms of the complex ion having no close contacts. Pairs of the {(tmedaH₂)Cl}_(∞/∞) columns are enclosed within a tube of complex ions (Figure 1(a)). The shortest Fe...Fe distances are 6.0871(3) (2−*x*, 1−*y*, 1−*z*), 6.7973(4) (*x*−1, *y*, *z*), and 7.2160(3) Å (¹/₂+*x*, ¹/₂−*y*, ¹/₂+*z*).

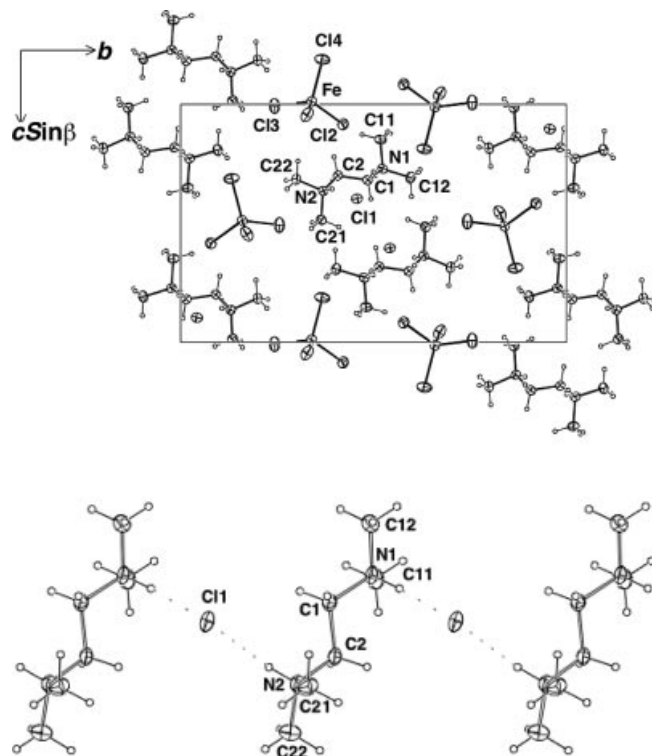


Figure 1 (a) Unit cell contents of (tmedaH₂)(FeCl₄)Cl, (1), projected down *a*.

(b) A hydrogen-bonded ...HtmedH...Cl...HtmedH...Cl... column, parallel to *a*.

Fe-Cl2-5 are 2.1919(4), 2.1923(5), 2.2026(5), 2.1862(5) Å, Cl2-Fe-Cl3-5 110.36(2), 107.90(2), 109.50(2); Cl3-Fe-Cl4,5 108.54(2), 110.04(2); Cl4-Fe-Cl5 110.47(2)°.

2. (ddmpH₂)[FeCl₄]Cl (2). Again, a full formula unit devoid of crystallographic symmetry, comprises the asymmetric unit of the structure (Figure 2(a)). Again, the role of the extended diprotonated cation is to link the uncomplexed chloride ions into a chain across the *ac* diagonal of the cell (Cl1...N,H14 (¹/₂+*x*, ¹/₂−*y*, ¹/₂+*z*) 2.991(3), 2.1; ...N,H(24)(*x*−¹/₂, ¹/₂−*y*, *z*−¹/₂) 3.057(2), 2.1 Å). (Figure 2b) The anion has no close hydrogen contacts, and, unsurprisingly, is disordered. The dihedral angle between the aromatic planes of the cation is 72.32(8)°; C-N-C angle sums are 338.1, 336.5°. The shortest Fe...Fe distances are 7.3799(8) (*x*−¹/₂, ¹/₂−*y*, *z*−¹/₂) and 7.677(1) Å (¹/₂−*x*, *y*−¹/₂, ¹/₂−*z*).

3. (enH₂)[FeCl₅(OH₂)] (3). A full formula unit, devoid of crystallographic symmetry, comprises the asymmetric unit

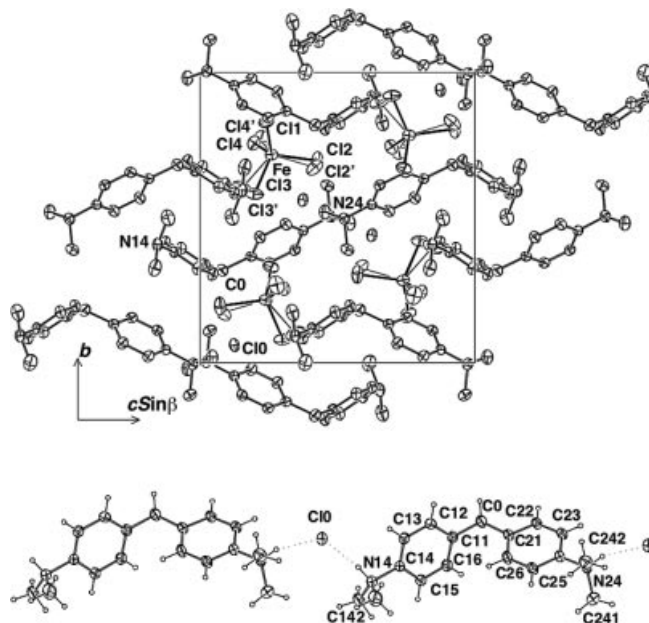


Figure 2 (a) Unit cell contents of (ddmpH₂)(FeCl₄)Cl, (2) projected down *a*.

(b) A hydrogen-bonded ...HddmpH...Cl...HddmpH...Cl... strand. Within the complex anion, Fe-Cl (fragment) distances range between 2.142–2.213(7) Å.

of the structure, which, overall, is chiral, the chirality somewhat ambiguously defined in the refinement, seemingly in consequence of the pseudo-centrosymmetric nature of the structure (Figure 3). The structure of the anion (Table 1), although similar to those defined in other studies [5, 14], appears less susceptible to deformation by hydrogen-bonding and other effects than elsewhere. The distances Fe-Cl2–4, all *trans* to other Fe-Cl bonds are closely matched but Fe-Cl1 is aberrantly short; the shortening of Fe-Cl5 may be ascribable to hydrogen-bonding elsewhere or a *trans*-influence arising from the water molecule oxygen atom. The hydrogen atoms of the latter interact with chlorine atoms of neighbouring anions: H1A0...Cl2 (*x*−¹/₂, ¹/₂−*y*, 2−*z*) 2.43(2), H1B0...Cl5 (*x*−1, *y*, *z*) 2.45(2) Å, the NH₃ hydrogen atoms all interacting with anionic chlorine atoms at distances (est.) of 2.51–2.69 Å, excepting a shorter contact H2A...Cl3 (¹/₂+*x*, ¹/₂−*y*, 2−*z*) 2.36 Å, and noting also H2B equidistant between Cl1,2 (*x*, 1+*y*, *x*) 2.62, 2.66 Å, offering no immediate explanation for the shortness of Fe-Cl1, or the distortions of nearly ten degrees in one of the *trans* angles, a concomitant of a more than five degree distortion in one of the *cis*. There are four quasi-equivalent (reflecting the pseudo-symmetry) Fe...Fe distances (to (*x*±1, *y*, *z*), (*x*±¹/₂, ¹/₂−*y*, 2−*z*) 6.8796(6), 6.8996(4) Å.

Magnetic properties

The magnetic properties of complexes (tmedaH₂)[FeCl₄]Cl (1), [ddmpH₂][FeCl₄]Cl (2) and (enH₂)[FeCl₅(OH₂)] (3) were determined over the temperature range 1.8–300 K.

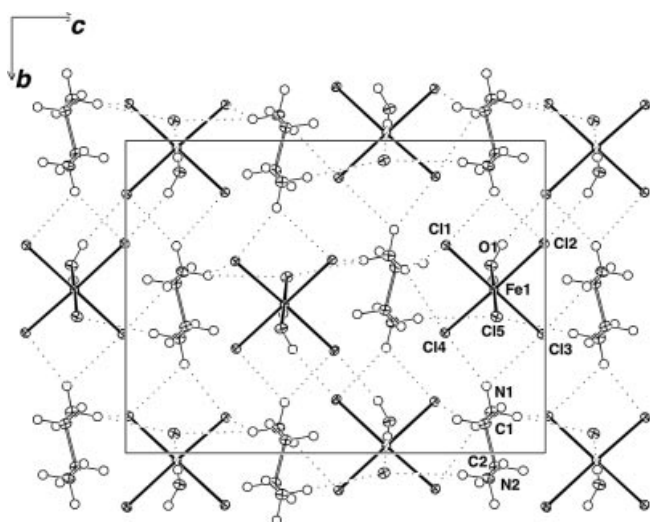


Figure 3 Unit cell contents of $(\text{enH}_2)[\text{FeCl}_5(\text{OH}_2)]$, (3) projected down a , showing hydrogen-bonding interactions.

Table 1 Anion structure $(\text{enH}_2)[\text{FeCl}_5(\text{OH}_2)]$ (3)

r is the iron-ligand atom distance /Å; other entries in the matrix are the angles subtended by the relevant atoms at the head of the row and columns

r	Cl2	Cl3	Cl4	Cl5	O1
Cl1	2.3268(2)	91.60(1)	174.24(1)	89.24(1)	93.08(1)
Cl2	2.3742(3)		89.73(1)	170.65(1)	94.45(1)
Cl3	2.3780(3)			88.55(1)	92.40(1)
Cl4	2.3750(3)				94.80(1)
Cl5	2.3439(3)				84.09(2)
O1	2.1698(8)				178.89(3)

In the cation C1-C2,N1 are 1.516(2), 1.487(1) and C2-N2 1.487(1) Å; N-C-C angles are 109.70(9), 109.81(8)°. O-H1A,B0 are 0.83(2), 0.81(2) Å.

Plots of magnetic susceptibility χ_M and the $\chi_M T$ product vs. T are given in Figures 4(a), (b) and (c), respectively.

The value of $\chi_M T$ at 300 K for complex 1 equals $4.27 \text{ cm}^3 \text{ mol}^{-1} \text{ K}$ (5.85 B.M.), the value of this product decreasing only slightly as the temperature is lowered. Below 50 K a more evident decrease in its value is observed with continuous decrease of the temperature, reaching $2.42 \text{ cm}^3 \text{ mol}^{-1} \text{ K}$ (4.41 B.M.) at 1.8 K. The decrease in value in the lowest temperature range is caused by antiferromagnetic interactions between Fe^{3+} ions, transmitted through the crystal lattice.

In this situation the magnetic data were fitted using the susceptibility equation for $S = 5/2$, (eq.(1)). To elucidate the significance of exchange between the Fe^{3+} ions in the crystal lattice, a molecular field correction term was also included (eq. (2)) [12]:

$$\chi_M = \frac{N\beta^2 g^2}{3kT} S(S+1) \quad (1)$$

$$\chi_M^{\text{corr}} = \frac{\chi_M}{1 - \frac{2zJ'}{N\beta^2 g^2}} \cdot \chi_M \quad (2)$$

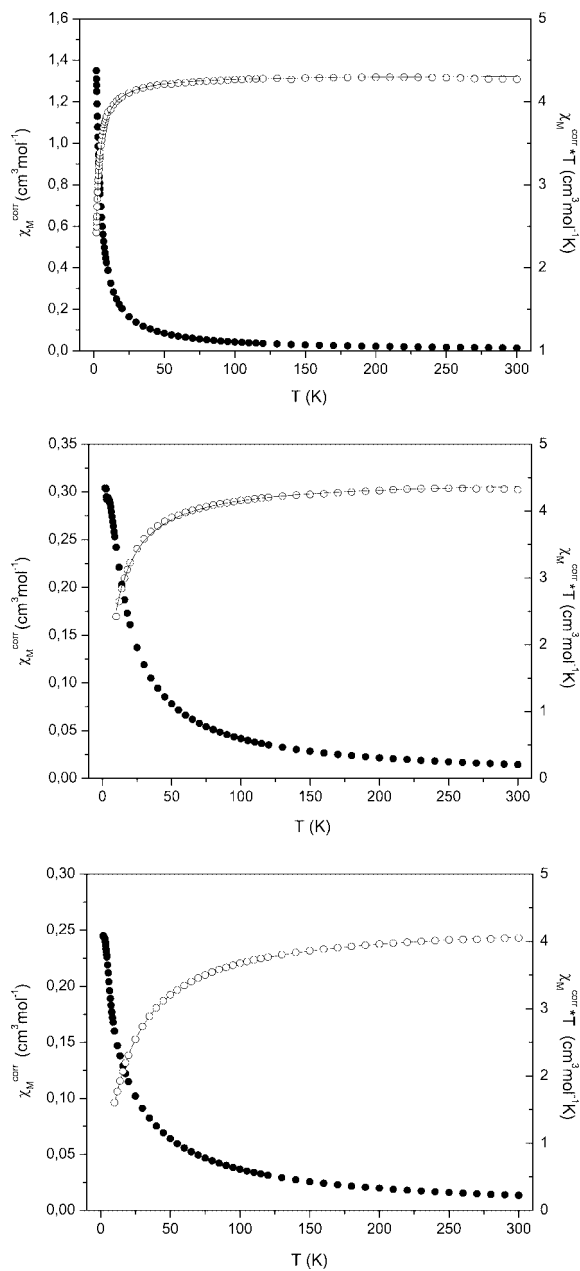


Figure 4 (a) Temperature dependence of experimental χ_M (●) and $\chi_M T$ (○) vs. T for (1). The solid line is the calculated curve for $\chi_M T$. (b) Temperature dependence of experimental χ_M (●) and $\chi_M T$ (○) vs. T for (2). The solid line is the calculated curve for $\chi_M T$. (c) Temperature dependence of experimental χ_M (●) and $\chi_M T$ (○) vs. T for (3). The solid line is the calculated curve for $\chi_M T$.

where N is Avogadro's number, g is the spectroscopic splitting factor, β is the Bohr magneton, k is the Boltzmann constant, zJ' is the intermolecular exchange parameter and z is the number of nearest neighbor Fe^{III} atoms. The least-squares fit of the experimental data using these equations was limited from 10 to 300 K and gives $zJ' = -0.18 \text{ cm}^{-1}$ and $g = 2.03$, as indicated by the solid curve in Figure 4(a). The agreement factor R is equal to 6.68×10^{-5} . The criterion used in determination of the best fit was based

on minimization of the sum of squares of the deviations $[(\chi_M T)^{obsd} - (\chi_M T)^{calcd}]^2 / [(\chi_M T)^{obsd}]^2$

The complexes **2** and **3** have similar magnetic behavior. For **2**, the value of $\chi_M T$ at 300 K equal $4.32 \text{ cm}^3 \text{ mol}^{-1} \text{ K}$ (5.88 B.M.) and the value of the $\chi_M T$ product decreases with temperature lowering to $0.55 \text{ cm}^3 \text{ mol}^{-1} \text{ K}$ (2.09 B.M.) at 1.8 K. For complex **3** the value of $\chi_M T$ at 300 K equals $4.05 \text{ cm}^3 \text{ mol}^{-1} \text{ K}$ (5.70 B.M.). The value of the $\chi_M T$ product decreases with temperature lowering to $0.441 \text{ cm}^3 \text{ mol}^{-1} \text{ K}$ (1.88 B.M.) at 1.8 K.

The susceptibility curves of all complexes exhibit no maxima indicating the presence of antiferromagnetic ordering with a Néel temperature (T_N), but in the cases of **2** and **3**, some slight curvature in the plots may suggest that a maximum can appear below 1.8 K.

Similarly, the magnetic data for **2** and **3** were fitted using the simplest susceptibility equation for $S = 5/2$ with a molecular field correction (Eq.(1) and (2)) [12]. The best-fit parameters in the 10 to 300 K range are $zJ' = -0.94 \text{ cm}^{-1}$ and $g = 2.02$ ($R = 3.43 \times 10^{-5}$) for complex **2**, as indicated by the solid curve in Figure 4(b), and for **3** these are $zJ' = -2.04 \text{ cm}^{-1}$ and $g = 1.98$ ($R = 3.07 \times 10^{-6}$), as indicated in Figure 4(c).

The values for the Curie and Weiss constants determined from the relation $1/\chi_M T = f(T)$ over the temperature range 50 – 300 K are equal to $4.30 \text{ cm}^3 \text{ mol}^{-1}$ and -0.73 K for complex **1**, $4.45 \text{ cm}^3 \text{ mol}^{-1}$ and -6.92 K for complex **2**, and $4.28 \text{ cm}^3 \text{ mol}^{-1}$ and -16.6 K for complex **3** (Table 2). The negative values of Weiss constants and intermolecular exchange parameters obtained from the calculation confirm the occurrence of weak antiferromagnetic interactions between the iron centers in the crystal lattice.

Table 2 Magnetic data for complexes **1–3**.

Compound	<i>g</i>	<i>zJ'</i> cm^{-1}	<i>R</i>	T_N K	Curie constant $\text{cm}^3 \text{ mol}^{-1} \text{ K}$	Weiss constant K
(tmedH ₂)[FeCl ₄]Cl (1)	2.03	-0.18	6.68×10^{-5}	–	4.30	-0.73
(ddmpH ₂)[FeCl ₄]Cl (2)	2.02	-0.94	3.44×10^{-5}	–	4.45	-6.92
(enH ₂)[FeCl ₄ (OH ₂)] (3)	1.98	-2.04	3.07×10^{-6}	–	4.28	-16.6

The variation of the magnetization *M* versus the magnetic field *H* for the complexes **1**, **2** and **3** at 2 K (Figure 5) clearly supports the occurrence of weak antiferromagnetic interactions. As the magnetic field increases, the *M* versus *H* curve for **1** indicates a linear relation up to ~1 Tesla and then shows a sinusoidal variation up to 5 Tesla, with saturation at *M* = 4.78 B.M. The *M* versus *H* curve for **2** is linear in the whole field range and indicates a value of magnetization 2.94 B.M. at 5 T. Magnetization of the sample even at 5 Tesla and 2 K is well below the saturation value of 5 B.M. expected for an $S = 5/2$ ground state with $g = 2$ in the absence of zero-field splitting or antiferromagnetic coupling. The *M* versus *H* curve for **3** is linear in the whole field range and indicates a value of magnetization 1.61 B.M. at 5 T, also well below the saturation value.

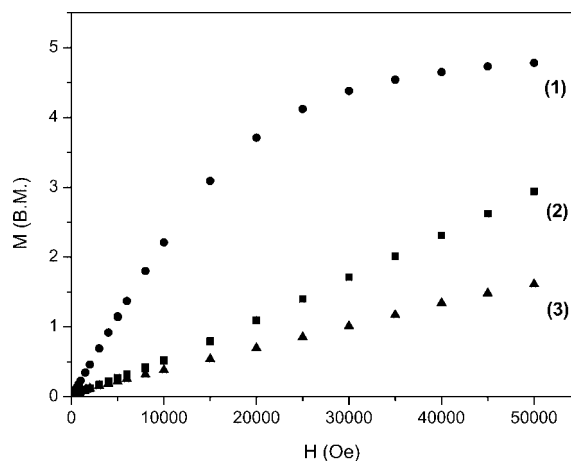


Figure 5 Field dependence of the magnetization at 2 K for complexes (**1**), (**2**) and (**3**).

The foregoing results of the magnetic susceptibility measurements of the compounds show some differences in magnetic properties dependent on the kind of organic counterion. The presence of the bulky cations results in a diamagnetic dilution due to increasing distance between the paramagnetic Fe^{III} atoms, and the magnetic interaction might be transmitted by the crystal lattice. This manifests itself in a decrease in the intermolecular exchange parameter and the value of the Weiss constant. In the case of the (ddmpH₂)²⁺ ion complex **2**, a stronger antiferromagnetic interaction is observed between the Fe³⁺ ions than for the complex with the tetramethylethylenediammonium cation. The small values of the intermolecular exchange parameters suggest only weak antiferromagnetic interactions between the magnetic atoms of Fe^{III}. Although the ethylenediammonium cation is less bulky and unhindered (and leads to a different structure) than is the case for (ddmpH₂)²⁺ and (tmedaH₂)²⁺, the Fe^{III} atoms are still quite far apart. The Néel temperature for the ammonium ion analogue is reported to be around 7 K [13] and the ordering temperatures of the alkali metal salts also have been described as “unusually high” [14a], so it is possible that the more bulky nature of the ethylenediammonium cation compared with the M⁺ cations might be the dominant factor in this case. For the recently reported diethylenetriammonium aquapentachloroferrate(III), however, T_N is 2.70 K [15], and it may be that a combination of cation flexibility and its greater ability for hydrogen bonding permits somewhat better exchange than in the (enH₂)²⁺ case, but the factors remain unclear.

The mechanism of superexchange pathways between the electrons of iron(III) in the systems studied appears to be that, in view of lack of bridging ligands between the Fe³⁺ ions, the most probable interaction pathway is likely to occur through orbitals of neighboring chloride ligands, namely Fe–Cl⋯Cl–Fe or additionally via the free chloride ions [7, 16]. For complex **3**, the interaction pathway could also involve the water ligand. Since the Fe⋯Fe distances in the

examined compounds are all rather long (*vide supra*), it is to be expected that the coupling between electrons of the Fe^{3+} ions in the systems will be weak.

The EPR spectra of all the complexes at room temperature, 77 K and 4.5 K indicate a single isotropic line only, characteristic for an unresolved $^6\text{S}_1$ state and a transition $+1/2 \leftrightarrow -1/2$ (Table 3). The EPR spectrum of the Fe^{III} atom in a tetrahedral crystal field is strongly dependent on the character of the tetrahedral distortion and the composition of the coordination sphere (types of ligands). For complexes containing the symmetric anionic form $[\text{FeCl}_4]^-$ good quality, intense signals of the EPR spectra are observed, which are broadened with lowering temperature. Those of **3** are not very different, and may reflect the quasi-centrosymmetric nature of the ion in the structure.

Table 3 EPR data of complexes **1–3**.

Compound	293 K		77 K		4.5 K	
	g_{iso}	$\delta_{\text{Hpp}}^*/\text{Gs}$	g_{iso}	$\delta_{\text{Hpp}}^*/\text{Gs}$	g_{iso}	$\delta_{\text{Hpp}}^*/\text{Gs}$
(tmedH ₂)[FeCl ₄]Cl (1)	2.02 ₇	370	2.04 ₈	650	2.11 ₁	760
(ddmpH ₂)[FeCl ₄]Cl (2)	2.02 ₁	350	2.02 ₃	390	2.09 ₀	440
(enH ₂)[FeCl ₃ (OH ₂)] (3)	2.00 ₂	160	2.00 ₂	150	2.07 ₈	690

* peak to peak linewidth

References

- [1] See, for example, S. M. Nelson in *Comprehensive Coordination Chemistry*, G. Wilkinson, R. D. Gillard and J. A. McCleverty (Eds), volume 4, chapter 44, Pergamon Press, Oxford, 1987.
- [2] R. L. Carlin, *Magnetochemistry*, Springer-Verlag, Berlin, 1986.

- [3] M. B. Millikan, B. D. James, *J. Inorg. Nucl. Chem.* **1981**, *43*, 1175.
- [4] H. L. Friedman, *J. Am. Chem. Soc.* **1952**, *74*, 5.
- [5] B. N. Figgis, C. L. Raston, R. P. Sharma, A. H. White, *Aust. J. Chem.* **1978**, *31*, 2717.
- [6] a) J. A. Zora, K. R. Seddon, P. B. Hitchcock, C. B. Lowe, D. P. Shum, R. L. Carlin, *Inorg. Chem.* **1990**, *29*, 3302; b) R. Shaviv, C. B. Lowe, J. A. Zora, C. B. Aakeröy, P. B. Hitchcock, K. R. Seddon, R. L. Carlin, *Inorg. Chim. Acta* **1992**, *198–200*, 613; c) R. Shaviv, R. L. Carlin, *Inorg. Chem.* **1992**, *31*, 710; d) R. Shaviv, K. E. Merabet, D. P. Shum, C. B. Lowe, D. Gonzalez, R. Burriel, R. L. Carlin, *Inorg. Chem.* **1992**, *31*, 1724.
- [7] a) Z. Warnke, D. Wyrzykowski, G. Wawrzyniak, *Pol. J. Chem.* **2003**, *77*, 1121; b) D. Wyrzykowski, Z. Warnke, R. Kruszynski, J. Klak, J. Mrozinski, *Transition Met. Chem.* **2006**, *31*, 765.
- [8] H. Remy, H. J. Rothe, *J. Prakt. Chem.* **1926**, *114*, 137.
- [9] B. D. James, M. Bakalova, J. Liesegang, W. M. Reiff, D. C. R. Hockless, B. W. Skelton, A. H. White, *Inorg. Chim. Acta* **1996**, *247*, 169.
- [10] G. M. Sheldrick, SHELXL-97, 'A Program for Crystal Structure Refinement', University of Göttingen, Göttingen, Germany, **1997**.
- [11] E. König, *Magnetic Properties of Coordination and Organometallic Transition Metal Compounds*, Springer-Verlag, Berlin, 1966.
- [12] J. Samuel Smart, *Effective Field Theories of Magnetism*, W. B. Saunders Co., Philadelphia and London 1966.
- [13] S. R. Brown, I. Hall, *J. Mag. Magnet. Mat.* **1992**, *104–107*, 921.
- [14] a) A. J. Schultz, R. L. Carlin, *Acta Crystallogr.* **1995**, *B51*, 43; b) C. J. O'Connor, B. S. Deaver Jr., E. Sinn, *J. Chem. Phys.* **1979**, *70*, 5161.
- [15] B. D. James, J. Mrozinski, J. Klak, B. W. Skelton, A. H. White, *Z. Anorg. Allg. Chem.* **2007**, *633*, 974.
- [16] C. B. Lowe, R. L. Carlin, A. J. Schulz, C.-K. Loong, *Inorg. Chem.* **1990**, *29*, 3308.